Fall 12-2014

A Vegetation Analysis on Horn Island, Mississippi, ca. 1940 Using Characteristic Dimensions Derived from Historical Aerial Photography

Guy Wilburn Jeter Jr.
University of Southern Mississippi

The University of Southern Mississippi

A VEGETATION ANALYSIS ON HORN ISLAND, MISSISSIPPI, CA. 1940 USING CHARACTERISTIC DIMENSIONS DERIVED FROM HISTORICAL AERIAL PHOTOGRAPHY

by

Guy Wilburn Jeter Jr.

A Thesis
Submitted to the Graduate School
of The University of Southern Mississippi
in Partial Fulfillment of the Requirements
for the Degree of Master of Science

Approved:

Dr. Greg Carter
Committee Chair

Dr. Andy Reese

Dr. Skeeter Dixon

Dr. Karen Coats
Dean of the Graduate School

December 2014

ABSTRACT

A VEGETATION ANALYSIS ON HORN ISLAND, MISSISSIPPI, CA. 1940
USING CHARACTERISTIC DIMENSIONS DERIVED FROM
HISTORICAL AERIAL PHOTOGRAPHY

by Guy Wilburn Jeter Jr.

December 2014

Horn Island is part of the MS/AL barrier island chain in the northern Gulf of Mexico located approximately 18kn off the coast of Mississippi. This island's habitats have undergone many transitions over the last several decades. The goal of this study was to quantify habitat change over a seventy year period using historical black and white photography from 1940. Using present NAIP imagery from the USDA, habitat structure was estimated by using geo-statistics, and second order statistics, from a co-occurrence matrix, to characterize texture for habitat classification. Percent land cover was then calculated to determine overall land cover change over a seventy year period. The geo-statistic of the horizontal spectral variation (CV) of image textures was used to estimate habitat structure using a multi scale approach if any characteristics of habitat texture could be delineated from CV histograms. The classification met with a result of an 80% habitat map of Horn Island ca. 1940, at 21x21 window size proving, that CV can be used successfully to classify text of historical black and white imagery. It was, also proven that CV can be used to characterize relative patch size for slash pine woodland habitat types, but not for habitats with smaller horizontal variations (i.e., marsh, and dune herbland).

ACKNOWLEDGMENTS

The writer would like to thank Dr. Gregory A., as well as the other committee members, Dr. Andy Reese and Dr. Clifton Dixon, for their guidance and knowledge. Special thanks go to William Funderburk and Carlton Anderson for their help in data collection and processing.

TABLE OF CONTENTS

LIST OF TABLES

Table

LIST OF ILLUSTRATIONS

Figure

CHAPTER I

INTRODUCTION

Problem Statement

Several studies have successfully characterized regions of interests using hyper-spectral and multi-spectral imagery (Buddenbaum, Schlerf, & Hill, 2005; Ge, Carruthers, Gong, & Herrera, 2006; Hauta-Kasari, Parkkinen, Jaaskelainen, & Lenz, 1999; Lu & Weng, 2005). These studies use hyper-spectral and multi-spectral imagery textural features as proxy for classifying regions (e.g., habitat types, urban areas). These techniques use high spatial and radiometric resolution and allow researchers to devise methods with accurate and precise results. Historical black and white imagery, however, has less spectral information available compared to modern day satellite and aerial imagery, making present day image analysis techniques ineffective when characterizing spectral properties with black and white imagery. Black and white imagery is underutilized due to present day image analysis techniques that focus on modern hyper-spectral and multi-spectral image data sets.

However, the texture of an image can be used to analyze the spatial distribution of brightness values within a panchromatic image and has been successfully employed with the combination of spectral information, increasing classification accuracy of vegetation (Adam, Mutanga, & Rugege, 2010; Buddenbaum et al., 2005; Ge et al., 2006; Hauta-Kasari et al., 1999; Lu & Weng, 2005). Very few of these studies focus on the use of historical black and white imagery before Landsat (Browning, Archer, Asner, Mitchel, & Wessman, 2008; Caridade, Marcal, & Mendonc, 2008; Hudak & Wessman, 1998, 2001). Studies that analyze this type of imagery are important for the purpose of understanding

landscape change on a decadal scale due to historical aerial photography dates going back to the 1930s. Inferences on climate change can be made by analyzing the texture characteristics of vegetation. The objectives of this study were to evaluate habitat structure by using geo-statistics to represent characteristics indicative of a specific habitat type to assess the environmental mechanisms that affect the habitat types such as hurricanes and tropical storms events, changes in sediment budget, and relative sea-level rise. Other objectives were to create a habitat map of Horn Island, MS ca. 1940 and to assess land cover change from 1940 to 2010.

Barrier Islands and Impacts

Barrier Island Impacts

Along the Atlantic and Gulf coasts of the United States and Mexico exists the longest barrier island chain in the world (Figure 1) (Stutz & Pilkey, 2001). This barrier island chain makes up approximately 85% of the open ocean shoreline and is an important resource to the mainland areas (Lucas & Carter, 2010; Stauble, 1989; Stutz & Pilkey, 2001). These islands provide protection from everyday wind and wave energies and harbor biologically active areas such as sea grass beds and marine estuaries (Carter, Lucas, Biber, Criss, & Blossom, 2011; Peneva, Griffith, & Carter, 2008, 2011).The protection from every day wind and wave energies provided by barrier islands is critical for these types of environments to exist long term (Carter et al., 2011; Fonseca, 1996; Fonesca & Bell, 1998; Koch, 2001; Koch, Ackerman, Verguin, & Keilen, 2006). Barrier islands are economically significant with millions of people living and traveling to these islands; this promotes tourism and the local economy. Ocean City, Maryland is a traditional resort community located on a barrier island that experiences an influx in

population of around 8 million people on a yearly basis (Crompton, Lee, & Shuster et al., 2001). These islands are an important economic and natural resource to mainland areas where the geomorphic and ecological changes can be key indicators of climate change.

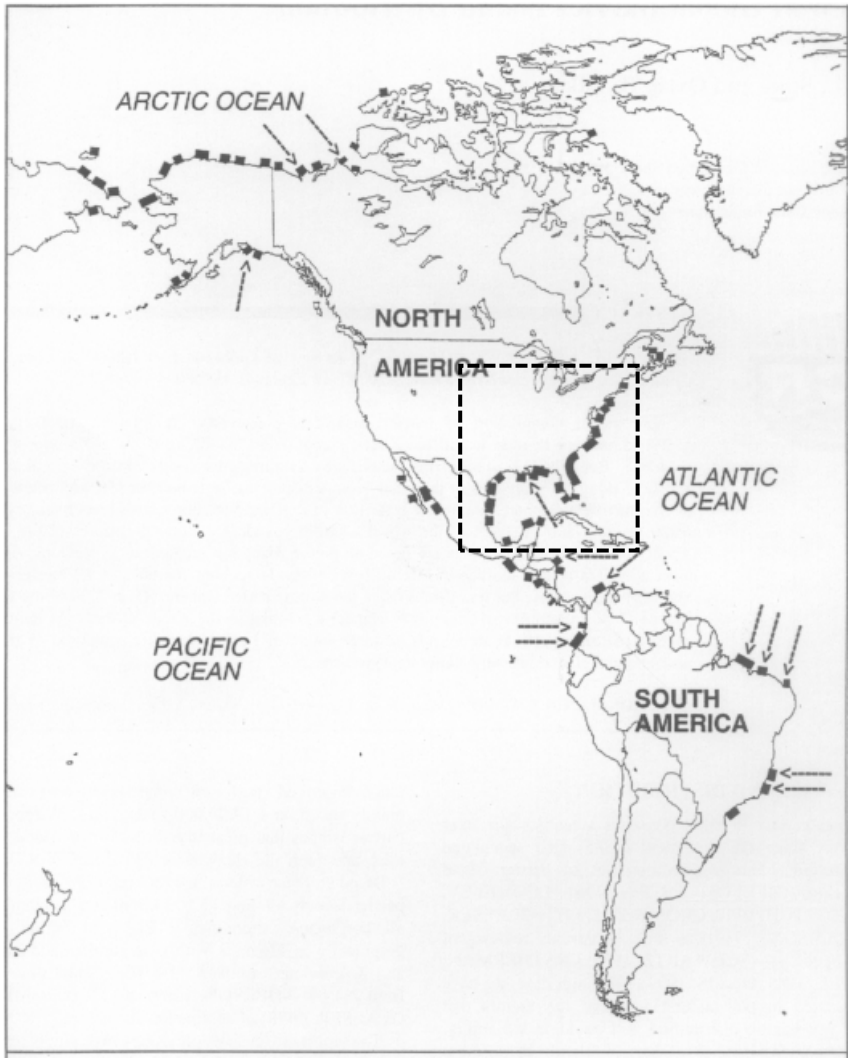

Figure 1. Map depicting barrier island distribution in the Western Hemisphere (Stutz & Pilkey, 2001). The black box indicates the world's longest barrier island chain along the Atlantic and Gulf Coasts of the Unites States and Mexico. The arrows indicate barrier islands formed by major river deltas.

It is important to recognize the harsh and dynamic environment that these islands endure. These islands are particularly sensitive to tropical storms and hurricanes, and relative sea-level rise (RSLR), and human impact (e.g., changes in sediment budget) (Day

et al., 2005; FitzGerald, Penland & Nummedal, 1984; FitzGerald, Fenster, & Argow, 2008; Morton, 2008; Otvos and Carter, 2008; Penland & Ramesy, 1990; Pilkey, 2003; Stutz & Pilkey, 2002, 2011). Depending on the geographic location, the size and strength as well as frequency of storms can either promote or degrade the stability of an island (Morton & Sallenger, 2003; Stone, Liu, Pepper, & Wang, 2004), playing a vital role in the reworking and natural restoration of barrier islands. Tropical storm and hurricane events also contribute to significant geomorphic changes resulting in land loss, erosion, salt water intrusion, and flooding (Morton, 2008; Otvos & Carter, 2008; Pilkey, 2003). Otvos and Carter (2008) reported hurricane effects for the MS/AL barrier chain. They reported island fragmentation, a reduction to sub-tidal shoal platforms, erosive, and aggradation affects from hurricane Katrina in 2005 for the Mississippi /Alabama (MS/AL) barrier island chain. These storm events can also affect vegetation by sand over wash, salt water toxicity, and flooding as well as by (Cahoon, Hensel, Spencer, Reed, McKee, & Saintilan, 2006; Otvos & Carter, 2008; Wang, Kirby, Haber, Horowitz, Knorr, & Krock, 2006; killing off or burying primary species, changing the landscape and in some the cases for a given area (Lucas & Carter, 2008).

Sea-level rise also plays an important role in the development of a barrier island system. Sea-level rise is a function of the ocean surface controlled by 1) volume of ocean water; 2) volume of the ocean basins; and 3) distribution of the water and the land surface (FitzGerald et al., 2008; Willis, Chambers, Kou, & Shum, 2010). The rate at which global sea levels have been rising is around 1.7 mm yr^{-1} (Cabanes, Cazenave, & Le Provost, 2001; Church & White, 2006; Douglas & Peltier, 2002; Holgate & Woodworth, 2004) where sea-level rise trends have been rising for several thousand years on the Atlantic

and Gulf coasts of the United States. Several studies have concluded that the sea-level has consistently risen for several thousand years and still is rising at a slower rate starting approximately 4,000 years ago (Douglas & Peltier, 2002; Hoyt, 1967; Penland et al., 1990; Penland, McBride, Williams, & Suter, 1991; Pilkey, 2003; Stanley & Warne, 1994; Tornqvist et al. (2004).

Studies have confirmed, because of this change in sea-level, barrier islands along the Atlantic and Gulf coasts of the United States have retreated landward, and that sediment supply is a key factor in the stability and longevity this coastal environment (FitzGerald et al., 2008; Hoyt, 1967; Morton, 2008). Sediment supply plays an important role in the support of barrier island and wetland areas allowing for low lying areas to accrete at a faster rate than sea-level rise (Brinson, Christoan, & Blum, 1995; FitzGerald et al., 2008; Morris, Sundareshwar, Nietch, Kjerfve, & Cahoon, 2002; Mudd, Howell, & Morris, 2009). Relative sea level rise (RSLR) is the combined effect in the Northern Gulf Coast, and has been consistently climbing four several thousand years (Tornqvists et al., 2004). The definition of RSLR can be defined, for this study, by including land and sea elevation changes over time. For example, barrier islands on the northern Gulf of Mexico experience coastal subsidence due to the weight of deposited sediments from river deltas compacting (Otvos, 1990). In particular Horn Island, of the Mississippi/Alabama (MS/AL) barrier island chain, has a subsidence rate of 5mm yr^{-1} (Lucas & Carter, 2010).

Human impacts such as the channelization of an inlet can cause significant land loss and in some cases a reduction in land area up to 60% in the case of East Ship Island in the MS/AL barrier chain (Lucas & Carter, 2010; Morton, 2008). Shipping lanes developed to the west of Petit Bois, Horn, and East and West Ship Island have caused a

net loss in land area dating back 158 years (Morton, 2008). This land loss can be exacerbated by relative sea-level rise due to coastal subsidence rates of the surrounding area (Lucas & Carter, 2008; Morton, 2008). Morris Island, SC is another example of humans impacting the development of barrier islands. In the late 1800s after the Civil War, jetties were constructed to boost the economy of Charleston Harbor by the U.S. Army Corp of Engineers. With these jetties in place tides could no longer supply the ebb tidal delta that was the sediment supply for islands south of Charleston Harbor. This led to a major landward retreat to the mainland which was most evident on Morris Island, SC. This can be seen due to the Light House that was historically on the island but is now sitting 1,550 ft. offshore (Pilkey, 2003).

Barrier Island Requirements, and Formation

Barrier islands largely exist, on the North America continent, along the trailing edge of the North American tectonic plate (Pilkey, 2003; Stutz & Pilkey 2001, 2011). A gentle sloping continental shelf, a consistent sediment supply, rising sea-level, wind and wave energies, and tidal influences are five requirements that are the key to barrier island development along the Atlantic and Gulf coasts of the United States (Oertel, 1985; Pilkey, 2003). Tidal and wave energies affect an Atlantic section of the world's largest barrier island chain known as the Georgia Bight (Davis & Hayes, 1984; Hayes, 1994; Pilkey, 2003). The higher wave energy along the North Carolina coast causes barrier islands to be longer and thinner with very few inlets spaced far apart; conversely barrier islands in Georgia and South Carolina are affected by larger tidal energies causing, many inlets between islands spaced closed together (Hayes, 1994; Pilkey, 2003). Islands along

the Gulf Coast of the United States receive lower tide and wave energies compared to the Atlantic.

There are several accepted theories of barrier island formation. These theories are as follows: submerged offshore bars where sediment is deposited and wave action allows for the sand bar to break the water surface, sand spit formation on the mainland is broken off by wind and wave energy creating a barrier island, and submergence of ridge complexes where water eventually surrounds sand platforms, and finally barrier islands formed by deltaic sediment deposits (Hoyt, 1967, 1968; Otvos, 1985; Schwartz, 1971; Swift, 1975). It is important to understand that barrier islands form under specific conditions unique to each island. These formation theories give a broad geomorphic descriptions that are common in a coastal setting.

Remote Sensing and Image Analysis

Remote Sensing

Recent developments in remote sensing technology have given rise to airborne and satellite platforms such as hyper-spectral imagery, multi-spectral imagery and LIDAR have given rise to new techniques of image analysis (Jensen, 2007). These technologies actively and passively use light to measure spectral and distance differences within a landscape or area study. Hyper-spectral and multi-spectral imagery passively sense variations of spectral reflectance at various wave lengths. These sensors can be used for several different ecological and physical applications and present multiple advantages to researchers. One key advantage of hyper-spectral and multi-spectral imagery is the scale at which spectral data can be collected. Multi-spectral satellite sensors such as Landsat TM (Thematic Mapper), MODIS, and SPOT satellites allow

researchers global data coverage at a relatively high spatial resolution (10m-80m) (meter). Scientists have successfully exploited this advantage in quantifying land changes and land use on a regional scale in some instances on a global scale (Carlson & Arthur, 2000; Stutz & Pilkey, 2001; Shalaby & Tateishi, 2007; Vogelmann, Sohl, & Howard, 1998).

Other benefits include the development of aerial platforms and the capability to select specific bandwidths for analysis, particularly vegetation analysis. Airborne platforms usually have much higher spectral and spatial resolution than satellite platforms (10 - <1m) (meter) and exhibit spectral resolutions as accurate as 10nm (nanometers). These platforms can also be deployed faster and give investigators the ability to collect in situ data. Hyper-spectral and multi-spectral data give researchers the capability to select specific bandwidths for vegetation analysis.

Vegetation studies using hyper-spectral spectroscopy chose specific bandwidths to measure spectral reflectance differences of different species of plants on a leaf level. These studies investigated the spectral characteristics of plants species on, at a leaf level, relationships with the red and infrared range of the electromagnetic spectrum and plant stress (Carter, 1993; Horler, Dockray, & Barber, 1983a; Jensen, 2007). Studies concerning the spectral characteristics of a given leaf, showed an increase in the near infrared part of the spectrum where leaves would reflect a 40 to 60% of incident near-infrared light from the structure of the leaf with the rest being transmitted thought the leaf and could be (Jensen, 2007).

Understanding the physiology of a given plant is important, particularly the characteristics of pigments such as chlorophyll a or b. When a plant is under stress,

chlorophyll production decreases thereby increasing the reflectance in the visible spectrum of the plant (Jensen, 2007). When chlorophyll production is down, the amount of light absorbed in the blue and red absorption bands is decreased (Carter, 1993; Jensen, 2007). This will make the plant reflect more light in the visible spectrum (Carter, 1993). Infrared can detect plant stress only when the plant has severe dehydration (Jensen, 2007).

Advantages of New Remote Sensing Technology

With the availability of real time data and the ability of satellite and airborne platforms to repeatedly collect data accurately and consistently, is yet another advantage exploited by researchers. Investigators have been successful in quantifying change over time for this very reason. Satellites such as Landsat TM have been in operation since 1972 which offers consistent coverage of an area of interest for several decades (Jensen, 2007). This can be useful in determining vegetation response to climate and landscape change. Remote sensing aerial platforms can also collect images at a researcher's chosen time and generally have much higher spatial resolution than satellite imagery. With these recent developments, advantages in fusion of multiple remote sensing data sets are a common approach of analysis. The focus of data fusion is to incorporate different data sets to extract more information than can be determined from one sensor (Pohl & Van Genderen, 1998). The fusion of hyper-spectral and LIDAR is an excellent example of how fusing data sets can provide a better interpretation of vegetation, giving a third dimension (canopy height) accurately identifying specific characteristics of, vegetation structure (Jensen, 2007).

Historical Black and White Imagery

These advantages of new remote sensing technology are very useful to scientists and researchers alike. The stigma of using the newest and best remote sensing equipment has caused many investigators to overlook the wealth of spatial information in historical black and white aerial photography, leaving few studies involving the texture analysis of historical black and white imagery (Hudak & Wessman, 1998, 2001) Historical black and white aerial photography can be difficult to interpret for several reasons.

This type of imagery is often several decades old, and deterioration of the physical image is an issue that can affect the outcome of analyses related to classification. Access to historical black and white imagery is relatively simple since the United States Geological Survey (USGS) has archived over 2 million historical black and white images and made them available for purchase (USGS); however, images are limited to the areas where they were taken. Historical contextual data for the surrounding area of the image may be difficult to acquire. Finally, due to the spectral information available in black and white imagery, the methods used to analyze multi-spectral or hyper-spectral imagery cannot be employed.

This study focused on the use of historical black and white imagery to achieve a decadal scale view of changes in habitat environments of Horn Island, MS over a seventy year period. The main purpose for this research was to devise a geo-statistical method to successfully determine and classify habitat types, using image texture black and white imagery, and to create a habitat map ca. 1940 of Horn using (USGS) historical black and white aerial imagery and 2010 (USDA) (NAIP) imagery at one meter spatial resolution. By conducting one of the most common and reliable, texture analysis techniques known

as co-occurrence matrix moving window analysis, a method was implemented for the classification of the historical 1940 USGS aerial imagery by using the geo-statistics calculated for the habitat types determined for the 2010 (NAIP) imagery as a reference for past habitat types.

This island was chosen as a study site for the location and barrier island dynamics that cause physical and ecological changes within a relatively short timeline as well as access to high resolution, quality imagery. Comparing imagery from 1940 and 2010 gave insight to the relationship of climate change and the processes that affect Horn Island (e.g., sea level-rise, major storm events, and sediment budget) through habitat changes of a barrier island ecosystem on a decadal scale.

Study Site

Horn Island is part of the MS/AL barrier island chain. This island chain formed around 4,000 years ago when the rate of sea-level rise slowed allowing for sediment coming from Mobile Bay, AL to be deposited on sand platforms. Due to prevailing wind and wave direction, these islands drift westward and toward the mainland. Horn Island is the largest island in the chain at around 1260 hectares (ha) in area and is located approximately 18km off the Mississippi coast (Lucas & Carter, 2008; Morton, 2008; Otvos, 1981; Pilkey, 2003) (Figure 2*).*

Past Environment

For the purpose of this study it is important to understand Horn Island's past habitats. In 1941 Pessin and Burleigh described Horn Island habitats in detail. Pessin and Burleigh (1941) described average temperatures in the summer and winter around 80.7˚F and 52.9˚F. Mean annual precipitation was estimated at 58 inches, and Horn Island was

13 miles long and approximately three quarters of a mile wide. The island consisted of ridges and swales with slash pine (*Pinus elliottii)* dominating the landscape. Pessin and Burleigh (1941) go on to describe heavily wooded areas consisting of slash pine (*Pinus elliottii)* along the borders of these ridges confined to the swales. Evidence of fire was noted on the western end of the island; however, Pessin and Burleigh determined that the island had not been burned in at least 20 years prior to 1941. They surmised this being the main reason for the dominance of slash pine over the extent of Horn with some cases over 5000 slash pines per acre.

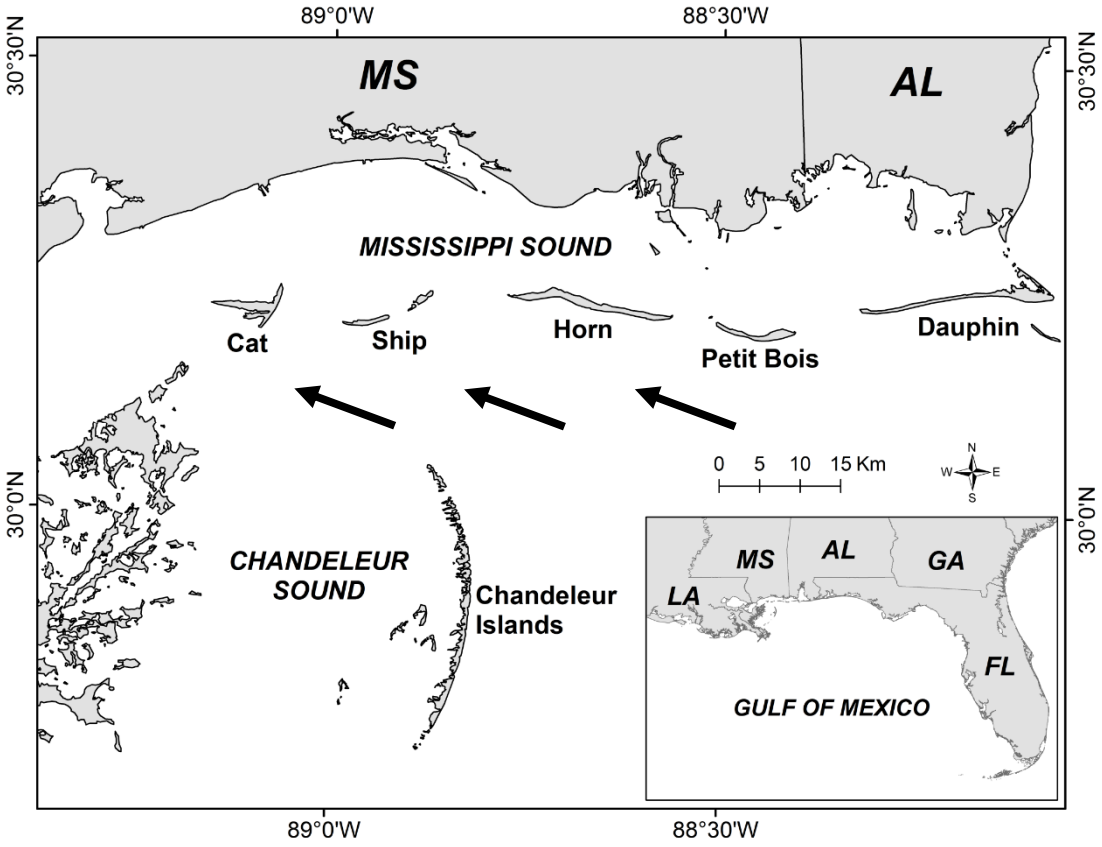

Figure 2. Map of MS/AL barrier island chain (Morton, 2008). The arrows indicate a westward drift of the island chain due to prevailing wind and wave direction.

These slash pines (*Pinus elliottii)* most likely had a small diameter breast height (d.b.h) (dog hair stands). They also describe the south side (Gulf) of the island as being

built up by wave action and windblown sediments. They describe the south western end of the forested areas of 20 feet wax myrtles being completely buried in windblown sediments. Wax Myrtle (*Myrica cerifera)*, Yaupon holly *(Ilex vomitoria)*, and beach rosemary *(Ceratiola ericoides)* are also common to this type of habitat. This type of habitat would be considered an estuarine shrub land. Dune habitats that would be considered dune herb land are located on the south side of Horn consisting of sedges, rushes, and grasses in high saline areas located on the south end of Horn where tides and over wash are common.

Present Day Environment

Recent descriptions of Horn Island tell a story of land loss due to sea level rise, coastal subsidence, hurricanes, and sediment entrapment including the westward current effecting sediment transportation out into the Gulf (Lucas & Carter, 2010; Morton, 2008; Otvos & Carter, 2008). Hurricanes such as Andrew and Katrina as well as sediment entrapment from shipping channels have significantly altered the land area of Horn Island with a reduction of overall area by 23% and estimated at 1245 hectares in area since 2010 Lucas and Carter 2010, 2012; Otvos and Carter 2008). The mean temperature for Horn Island, MS for winter and summer since Pessin and Burleigh (1941) has varied little with temperature at 12˚C (53.6˚F) and 27˚C (80.6˚F). As in the past Horn Island has similar habitat types of dune herb land, fresh and saltwater marshes, maritime forest (slash pine woodlands), lagoons, and freshwater ponds (Lucas & Carter 2010). Annual precipitation for present day Horn Island is 140cm (55.1 in).

Observations, Research Questions, and Objectives

When considering past habitat types on Horn Island, observations were made about the island itself and the use of historical black and white imagery. Several observations were considered concerning Horn Island 1) Since 1849 Horn Island has lost 19% of its overall land area. 2) The RSLR on Horn Island is around 7mm yr^{-1}. This gave rise to two questions regarding habitat type and change. 1) How has land loss affected the habitat types on Horn Island? 2) How has RSLR affected the habitat types on Horn Island over a seventy year period?

Observations concerning black and white imagery are as follows 1) The USGS has over 2 million digitally archived historical black and white images available to the public. 2) The literature suggests that not much research has been conducted using historical black and white imagery's spatial information for ecological research (Hudak & Wessman, 1998, 2001). 3) The spectral availability of historical black and white imagery is limited due to the technology accessible in 1940. 4) Only one historical habitat map is available for Horn Island but it only based on field observations from the late 1970s (Eluterius, 1979; Lucas & Carter, 2008). Two questions concerning black and white were asked 1) Can historical black and white imagery be used to create a reliable habitat classification map? 2) Can habitat characteristics be determined using black and white imagery?

CHAPTER II

IMAGE TEXTURE ANALYSIS METHODS

Image Texture

Texture

When determining significant visual patterns, humans easily recognize spectral, textural, and contextual features to interpret what one sees inside an image (Haralick & Shanmugam, 1973). Contextual features are data derived from information neighboring the area of interest (Haralick, 1979). Spectral properties are average tonal differences derived from numerous bands of the visible and infrared ranges throughout the electromagnetic spectrum where textural properties are the spatial variations of these tones (Coburn & Roberts, 2004; Haralick, 1979; Haralick & Shanmugam, 1973). The concept of tone is based on varying shades of grey level pixels in a photographic image (Haralick & Shanmugam, 1973) and in the case of Horn Island, black and white aerial photographs.

Texture vs. Tone

These two properties of differences in grey level tones (brightness) between pixels and the spatial variations of tone of those pixels are not independent of one another. Two key relationships have been observed between tone and texture; if a small region or patch of an image has small variations in grey-levels of features, then the principal property is tone. Secondly, if a small region in an image has a wide-ranging variation within a small region, then the dominant property is texture (Haralick, 1979; Haralick & Shanmugam, 1973).These two properties make up the tone and texture concept which can be used to describe and characterize textural features. These

relationships vary according to the size and structure of a region and the number of distinct features within an image (Haralick, 1979; Haralick & Shanumugam, 1973). Tone and texture are what humans instinctively notice and interpret everyday by using eyesight. Tone and texture can be used in a variety of approaches and applications in image analysis.

Texture Approaches

There are several approaches to texture image analysis to consider when classifying historical black and white imagery. 1) Structure based, 2) transform- based and 3) model based, and 4) statistical based (Bharati, Liu, & Mcgregor, 2004; Materka & Strzelecki, 1998; Van Gool, Dewaele, & Oosterlinck, 1985). Structure based approaches describe texture as the configuration of distinct primitives (tonal differences between pixels) that are regularly pattern. These patterns and texture features are defined by placement, as well as property (tonal and spatial) rules (Bharati et al., 2004; Carlucci, 1972; Haralick, 1979; Materka & Strzelecki, 1998; Zucker, Rosenfeld, & Davis, 1975). These rules can be defined by line segments or open or closed polygons (Carlucci, 1972). The probability of the chosen tonal and spatial properties and the location of the properties can be characterized as strong or weak textures of the properties and location in question (Haralick, 1979). Weak textures are textures that have weak spatial relationships between tonal pixel values. Strong textures can be defined as having systematic relationships and patterns between tonal pixel values (Haralick, 1979). An example of a weak texture would be the image texture of the random placement and tonal properties of flat bare sand environment, and an example of a strong texture would be the crop rows of an agricultural field.

Model based texture analyses develop an empirical model for each pixel based on weighted averages of pixel values within adjoining pixels (Baraldi & Parmiggiani, 1995; Materka & Strzelecki, 1998). Examples of texture model based analysis are autoregressive and fractal models. Autoregressive models assume that neighboring image pixel meaning pixel values are a weighted sum of neighboring pixel values (Haralick, 1979; Materka & Strzelecki, 1998). These types of models are employed in texture segmentation (characterization by object identification) applications or texture synthesis applications. Autoregressive methods observe the linear dependencies between pixel values. These linear dependencies are the parameters of an autoregressive model (Haralick, 1979). Fractal models are yet another option to assess the shape and direction of image textures. Fractals are mathematical expressions that describe the shape and nature of certain natural scenes. These expressions have dimensions which humans recognize as the smoothness or roughness of a surface (Pentland, 1984).

Transform based texture analysis such as wavelet transform and Gabor transforms translate images into to a different form using spatial frequency properties of pixel values at multiple resolutions (Arivazhagan & Ganesan, 2003; Bharati et al., 2004). There are some disadvantages when using these transforms for texture classification. For example when looking at Gabor transforms at different scales, different filters must be used to properly characterize textures (Arivazhagan & Ganesan, 2003; Bharati et al., 2004). This means that every time this type of transform is implemented at different resolutions it must be tuned or adjusted. These transforms such as Gabor and wavelet transforms have been used recently for object based texture analysis which is similar to structure based texture analysis.

Statistically based texture analyses are used with high order statistics to describe specific regions and their spatial frequency distributions. Techniques such as run length matrix also use high order statistics to portray coarse textures as having many contiguous pixels, having similar grey level tone and fine textures having a small number of contiguous pixels with similar grey level tones (Bharati et al., 2004; Van Gool et al., 1985). This method specifies lengths of pixel with certain grey tone values with in a matrix. This matrix determines the number of times a length is present in an image and in what direction this length is running (Haralick & Shanmugam, 1973; Van Gool et al., 1985).

Co-occurrence Matrix

One of the most cited and employed methods for statistical texture analysis is the Co-occurrence matrix. A co-occurrence matrix is an arrangement of frequencies of pixel pair elements. Pixel pair (i , j) can be defined as the number of times that a pixel value I is some distance and angle away pixel value j and the occurrence of variation between each pixel pair (Bharati et al., 2004; Haralick, 1979; Haralick et al., 1973; Honeycutt & Plotnick, 2008; Partio, Cramariuc, Gabbouj, & Visa, 2002). The co-occurrence matrix is calculated using angle and distance relations between neighboring pixels, eight neighbors for each pixel (Haralick, 1979; Haralick et al., 1973) (Figure 3). This type of statistical method implements second order statistics (e.g., Mean, Variance, Entropy, Energy, Contrast and Correlation) by assessing pixels at 0, 45, 90, and 135 degrees then moving a distance of one or more pixels and repeating the second order statistic calculation (Haralick, 1979; Haralick et al., 1973; Narashima et al., 2002) (Figure 3). Each record in a co-occurrence matrix relates to the number of occurrences of paired gray levels and can

be represented by 14 different second order statistics Bharati et al., 2004; Baraldi & Parmiggiani, 1995; Haralick, 1979; Haralick et al., 1973; Narashima et al., 2002; Partio et al., 2002).

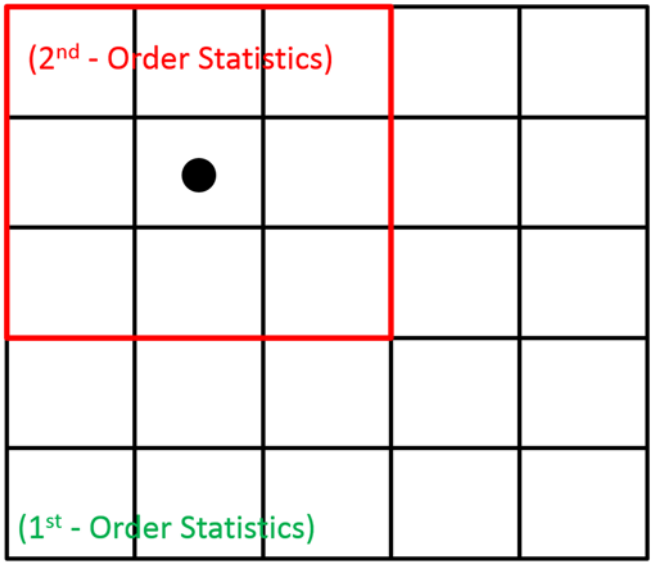

Figure 3. Co-occurrence matrix moving window analysis. This shows a 5x5 window size (outer box) second order statistics being calculated in the red box.

Texture Measures

Haralick defined 14 different second order statistics that could be used to estimate the similarity between gray level occurrences. The second order statistics that will be used for this research can be defined as such. Energy or Angular Second Moment (ASM) is a measure of texture homogeneity or uniformity; energy reaches its highest values when grey level distributions have a constant or intermittent repeated pattern (Haralick et al., 1973; Honeycutt & Plotnick, 2008). A homogenous image has few prevailing grey tone changes; therefore, the matrix has fewer values of larger magnitudes making ASM value larger. Entropy is measured as the disorder or complexity of an image. Entropy is highest when all elements of the co-occurrence matrix are equivalent. When the values of ASM and other features of a co-occurrence matrix are very small, this indicates entropy

being very large. So Entropy and ASM are inversely related (Baraldi & Parmiggiani, 1995; Haralick, 1979; Haralick et al., 1973; Partio et al. 2002).

Contrast measures the spatial frequency distribution differences between the highest and lowest pixel values of an adjoining set of pixels. This parameter is highly correlated with variance. Variance is a measure of heterogeneity between pixel neighbors. The more the pixels differ from the mean pixel values of, a specific window size, the higher the variance of that particular pixel related to its neighbors. Variance is highly correlated to the first order statistic of standard deviation (Baraldi & Parmiggiani, 1995). The mean parameter is the average pixel values of neighboring pixels aggregated to the center pixel of a specific a specific window size. The correlation parameter is articulated by a coefficient between to random pixel pixels within a co-occurrence matrix. This measurement can be expressed as the gray tone linear dependencies with in an image (Baraldi & Parmiggiani, 1995). This means high correlation values mean a strong linear relationship exists between grey levels of pixel pairs.

Spectral Information Available in 1940 Imagery

In order to properly analyze the 1940 and 2010 imagery the spectral information available from the historical black and white imagery must be addressed. Assumptions must be made about the spectral sensitivity of the film and camera equipment presumably used for the 1940 USGS aerial imagery. The film that was most commonly used in the time period of 1940 was Super XX and the K-17 vertical cartography camera with a six inch focal length (Katz, 1948). The spectral sensitivity of Supper XX only went to 660nm just before the infrared spectrum (Cox & Munk, 1954). Assumptions of the use of a yellow filter were considered in order to account for atmospheric scattering (Cox &

Munk, 1954; Katz, 1948). This type of filter was common practice in 1940. These assumptions are limited to the spectral information available for the 1940 imagery. This is why a textural approach was chosen for the classification of habitat type on Horn ca. 1940. Instead of measuring the spectral properties directly, the spatial distributions and differences in tone between each pixel were analyzed. In order to make comparisons the descriptions must be calibrated to similar spectral reflectance conditions before any texture analysis can be employed. It is of no use to conduct an analysis until the images are comparable. Devising calibration techniques to allow recent imagery to be comparable to historical black and white aerial photography would allow for a more accurate comparison to the 1940 imagery. By calibrating the 1940s and 2010 aerial imagery to percent reflectance an accurate a comparison can be employed using a textural moving window analysis.

Methods

Calibrating 1940 and 2010 Imagery

Historical black and white imagery of Horn Island, Mississippi, from 1940 was acquired from the USGS, and 2010 NAIP imagery was obtained from the USDA for analysis. Both image data sets are 1 meter in resolution. The 1940 imagery was geo-rectified to the NAIP 2010 imagery where both sets of imagery were masked by developing a region of interest (ROI) around 1940 and 2010 Horn Island shorelines using ENVI 4.8, which was used for all analyses in this study. This was done to reduce data processing time for any kind of analysis. The 2010 NAIP imagery has 4 bands that can be used: red, green, blue, and infrared. The red, green and, blue bands were averaged to create a panchromatic image of Horn Island ca. 2010. The infrared band was not used

because of the film sensitivity assumption of 660nm. The 2010 imagery was darker than the 1940 imagery; therefore, the 2010 image data set was stretched to the range of the 1940 imagery of BVs (0 to 242) (Figure 4). Thresholds were determined for the brightest areas of bare sand for each image data set to select bare sand BVs within a certain range. Four separate thresholds were created for each set of imagery. The threshold ranges, on an 8bit scale, for the 1940 imagery were as follows: 227-242; 229-242; 230-242, and 232-242. The threshold ranges for the 2010 imagery were as follows: 223-242; 225-242; 227-242; and 230-242 (Figure 5).

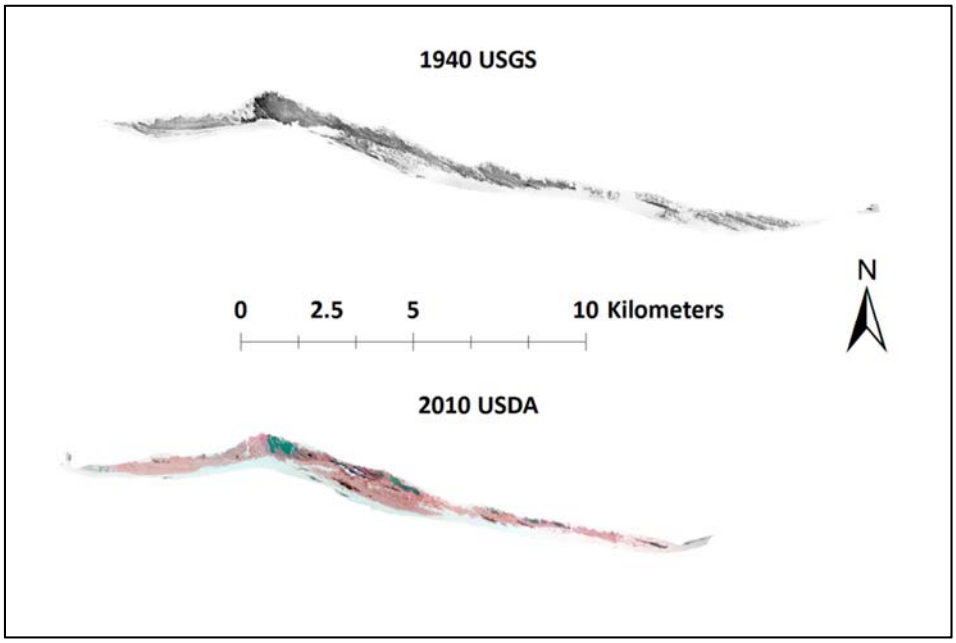

Figure 4. Imagery used for analysis. Top image: USGS historical aerial photography from 1940; Bottom image: USDA 2010 NAIP imagery. Both image data sets are 8 bit and have a one meter spatial resolution.

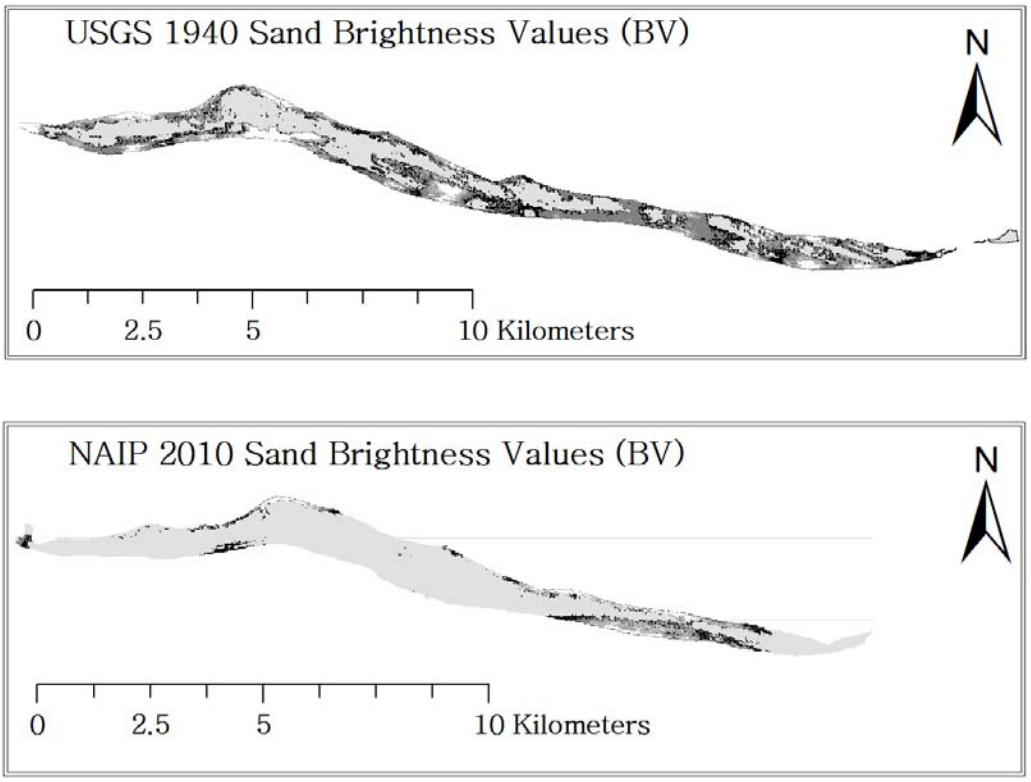

Figure 5. Brightest bare sand areas. Top Image: Brightest bare sand areas on Horn Island ca. 1940. Bottom Image: Brightest bare sand areas on Horn Island ca. 2010. The highest intensity areas are seen in white.

This allowed for a more accurate and precise measurement of the brightest bare sand areas in the image data sets. After the brightest bare sand areas were determined, 20,000 bare sand BVs were sampled from the concentrated values selected by the smallest threshold range for each image. 20,000 BVs were sampled to provide a good representation of the mean of the BVs sampled, varying only one decimal point of the brightest bare sand areas on Horn Island ca. 2010 (Figure 5). 1940 and 2010 Horn Island imagery correction factors were calculated by plotting 20,000 bare sand brightness values from each raw image against field mean spectral reflectance data of bare sand from Horn Island at a range of 500nm to 660nm (Figure 6). The field spectral data range was selected to account for a yellow filter being used as well as film sensitivity when the 1940

imagery was taken. The slopes calculated from this linear regression were used to calibrate to spectral reflectance.

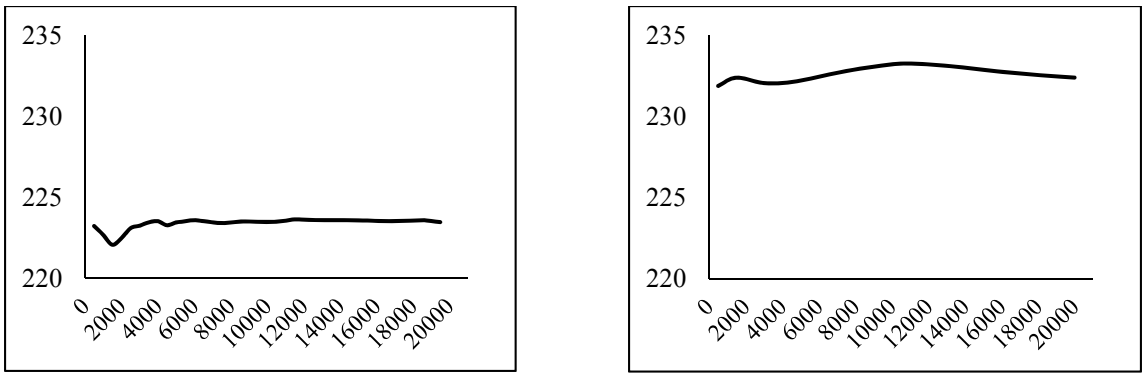

Figure 6. Mean pixel values for 2010 and 1940. 20,000 raw pixel values were sampled to determine the mean BV for bare sand for each image data set. Graph on left mean pixel values of 2010 NAIP imagery; Graph on right: Mean pixel values of USGS 1940 imagery.

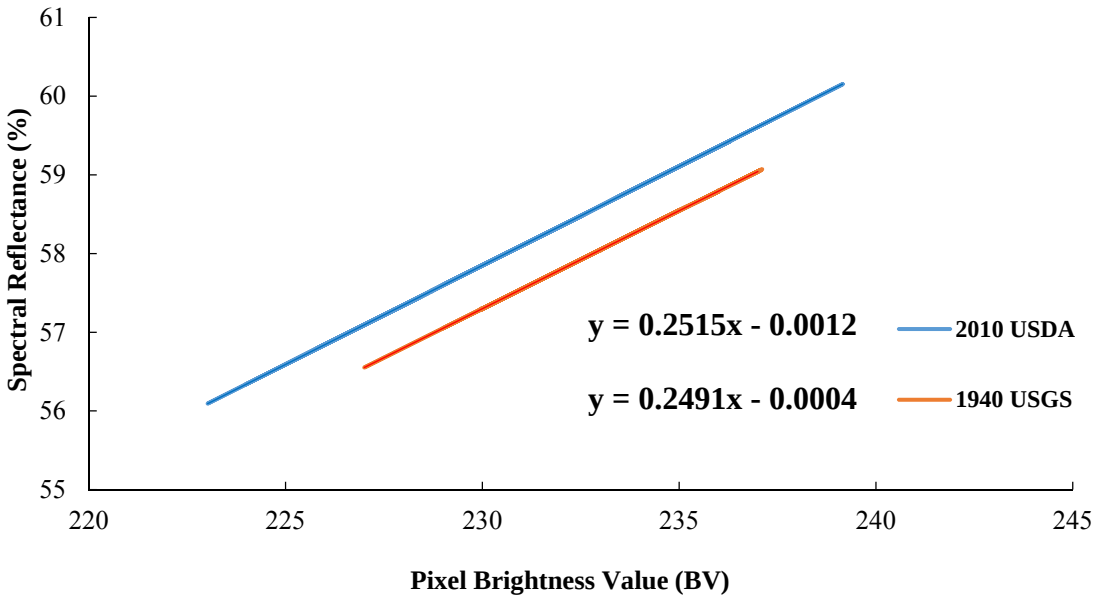

Figure 7. 2010 and 1940 linear regression. The slopes for each image data set were used to calibrate to percent reflectance. The slopes show precise standardization of the image data sets.

Determining Habitat Types for 2010 and 1940

Habitat Sampling for 2010

A 2010 GPS habitat database was created by the Gulf Coast Geospatial Center, using ArcMap 10.0 for the entire MS/AL barrier island chain. Each GPS point had information concerning primary and secondary plant species for the corresponding GPS points (Figure 7).

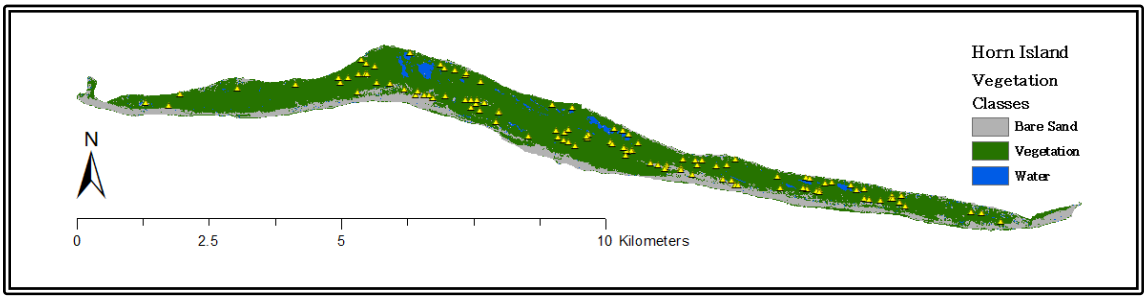

Figure 8. 2010 GPS geo-database. This map shows the randomly selected GPS points that were used to represent habitat types.

Along with the plant species information, oblique photographs for each cardinal direction (N, E, S, and W) were also attached to each point. Six habitat types were determined for the 2010 GPS database using the primary and secondary plant species and the definition of definitions of barrier island habitat types provided by the Mississippi Natural Heritage Program (2006), as a guide (i.e., bare sand, dune herb land, estuarine shrub land, marsh, slash pine woodland and water). The sample point density for Horn Island is one GPS point for every 7 hectares (ha). Additional sample points were added to each habitat type by using the cardinal directional photographs attached to each GPS point. This was done to increase the sample point density for each habitat type for the 2010 NAIP imagery and to increase accuracy for classification purposes. Sample points were selected by estimating one meter increments away from a range pole placed in each

photograph. One meter increments were chosen due to the spatial resolution of the image data sets being one meter.

1940 Horn Island habitat assumptions, coefficient of variation (CV), and sampling

Assumptions had to be made about the habitat structure of each habitat type for Horn Island ca. 1940. In order to predict and estimate habitat types for 1940 habitats it was presumed that the habitat structure (e.g., canopy size, and patch size) was the same for 2010 and 1940 Horn Island habitats. With this assumption a way to compare habitat structure that was independent of magnitude was needed in order to achieve comparable habitat types. The horizontal variation of the percent spectral reflectance or coefficient of variation (CV) images were created for 2010 and 1940 imagery by implementing a co-occurrence matrix moving window analysis for 5x5, 11x11, 15x15, 21x21, and 31x31 window sizes that were used to determine the CV values for habitat types.

CV images were created by running the co-occurrence matrix moving window analysis using the mean and variance algorithms for each window size and by implementing the band math tool in ENVI 4.8. By squaring the variance image a standard deviation image was produced. Then by dividing the standard deviation image by the mean image, a CV image can be calculated. By using the sample pixels collected for each habitat type from the 2010 GPS database, CV values for each 2010 habitat were determined and ranges of CV values were calculated using the minimum and maximum values for each habitat type ROI. 2010 CV value ranges were then used to determine thresholds for the 1940 imagery. These ranges are as follows: slash pine woodland, estuarine shrubland, marsh, and beach dune herbland. Pixel CV values were sampled for

the 1940 image data set based on these thresholds at comparable point densities to the 2010 imagery.

Maximum likelihoods using Texture Image Analysis and Percent Land Cover

Maximum likelihood (ML) classifications were made for each moving window size to determine which window size produced the highest overall accuracy using a confusion matrix. The Maximum likelihood method is a supervised classification method that assumes pixels within image bands are normally distributed and relies on the probability that a given pixel is correctly placed into one of the predefined classes (Jensen, 2007; Lucas & Carter, 2008; Peneva et al., 2008). This method uses training data, along with the pixels sampled, to take into account the variability of each distinct ROI or region of interest. This is one of the most reliable and accurate methods of classification which is why this method was used to classify each habitat type. A confusion matrix was employed to determine overall accuracies for each ML classification. Within the confusion matrix, commission and omission errors were used to determine how well the pixels were correctly placed in each habitat type. Commission error represents pixels that belong to another class that are labeled as belonging to the class of interest. Omission error represents pixels that belong to the ground truth class but the ML classification classified them as something else. In other words commission errors determined the error in the training pixels selected, and the omission error determined the error or the sample pixels that represent the GPS points and pixel selected using the cardinal directional photos.

Four other texture algorithms were employed for the ML classification. Entropy, ASM, correlation, and contrast. Overall accuracy for each ML classification was

calculated by a confusion matrix accuracy assessment. This matrix calculates overall accuracy by summing the number of pixels classified correctly and dividing it by the total number of pixels in the image. After determining the highest overall accuracies, the 21x21 window size ML was used to calculate percent land cover for each habitat type for both 2010 and 1940 imagery. Using class statistics in, ENVI 4.8, total land area in hectares of all habitat types were computed for Horn Island ca. 1940 and 2010. Then the total area of each habitat was divided by the total area of Horn Island for the corresponding time period to determine percent land cover for each habitat type.

Indicative Habitat Structure

Habitat structure was determined by using a similar multi scale method by employing different window sizes (5x5, 51x51, 101x101, 125x125, 151x151, 175x175 201x201, 225x225, 251x251, 300x300, and 350x350) using CV values for each habitat type to observe changes in horizontal spectral variation. To analyze habitat structure the mean CV values were calculated using the sample pixel values collected for each habitat type and displayed in bar graphs depicting a standard bell curve of horizontal variation of each habitat type. This method was employed to represent characteristics indicative of each habitat type at a specific window size. It was determined that analyzing habitat types in this matter could assist in revealing characteristics such as patch size or anything that may divulge any information concerning the structure of a habitat type by looking at the maximum variation of a habitat type at a given window size.

CHAPTER III

HABITAT CHANGE AND STRUCTURE, RESULTS AND DISCUSSION

Results

Overall accuracy results of ML classifications

The least accurate classification for the 1940 imagery was the 7x7 moving window analyses with an overall accuracy of 44.50%. The least accurate classification for the 2010 imagery was the 5x5 window size at an overall accuracy of 60.10%. A pattern developed showing an increase in accuracy with an increase in window size, with multiple peaks at the 11x11 and 21x21 window size with an overall accuracy at 80.1% for 1940 and 84.4% for 2010 for the 21x21 window size (Table 1). The literature suggests smaller window sizes cannot capture the true nature of texture in an image (Maenpaa & Pietkainen, 2003; Pacifici, Chini, & Emery, 2009). Several studies have seen similar patterns using texture for classification purposes (Coburn & Roberts, 2004; Hudak & Wessman, 1998, 2001; Pacifici et al., 2009).

Change Detection of Habitat Types on Horn Island

The total land area for Horn Island ca. 1940 was approximately 1550 (ha). The overall percent land cover percentage for each habitat type for Horn Island ca. 1940 is as follows: Slash Pine Woodland 25%; Estuarine Shrubland 21%; Dune Herbland, 12%; Marsh 4%; Bare Sand; 32%, and Water 7%. The total land area for Horn Island ca. 2010 was approximately 1262 (ha). The overall percentage of land cover for each habitat type of Horn Island ca. 2010 is as follows: Slash Pine Woodland, 9%; Estuarine Shrubland, 24%; Dune Herbland, 23%; Bare Sand, 13%, and Water, 6% (Table 2 and Figure 7).

Table 1

Overall Accuracies for 2010 and 1940 Window Sizes (%)

Window Size	2010 Horn Island	1940 Horn Island
5x5	75.37%	60.10%
7x7	82.82%	44.50%
9x9	86.88%	66.28%
11x11	88.85%	77.68%
13x13	83.02%	74.48%
15x15	80.17%	75.43%
17x17	80.73%	73.16%
19x19	82.49%	70.56%
21x21	84.36%	80.01%
31x31	67.50%	61.20%

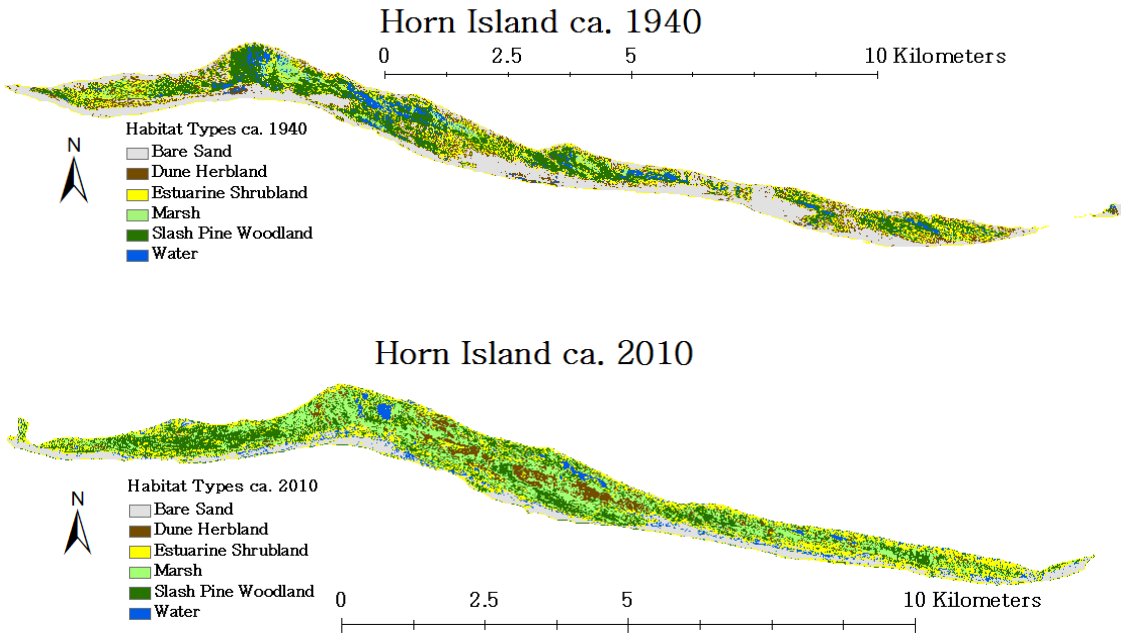

Figure 9. Horn Island 21x21 window size classifications. Top map: Horn island ca. 1940**;** Bottom map: Horn Island ca. 2010.

Slash pine woodland decreased in percentage of cover by 16%. Bare sand percentage also decreased by 19% where estuarine shrubland, dune herbland, and marsh habitats increased: estuarine shrubland by 4%, dune herbland by 11%, and marsh by 22%. The habitat type water remained fairly consistent, only decreasing in percentage land cover by 1%. Based on the observations made during this study it is possible to surmise what has caused these changes in habitat type over a seventy year period on Horn Island.

Table 2

Percent Land Cover for 1940 and 2010

Habitat Types	1940 % Land Cover	2010 % Land Cover
Bare Sand	32	13
Slash Pine Woodland	25	9
Estuarine Shrub Land	21	24
Dune Herb Land	12	23
Marsh	4	26
Water	7	6

Note. This table shows the 21x21 window size percent land cover results over a seventy year period. Notice the decrease in slash pine woodland and the increase in marsh habitats.

Habitat Structure

The slash pine woodland bell curve shows a maximum horizontal variation at a window size of 45x45 with a CV of 18.8 (Figure 8). Marsh and dune herbland habitats could not be successfully characterized (Figure 9 & 10). The estuarine shrubland CV histogram responded similarly as the marsh and dune herbland habitats (Figure 11). Bare sand characteristics were not developed due to CV values being constant throughout all

windows sizes. These curves were distinct provide spatial variation indicative of each habitat type.

Discussion

Calibration and Classification Method for Black and White Imagery

The goal to develop a method to classify the 1940 USGS Horn Island imagery was met with success. Given the results of the linear regression used to calibrate, the imagery reveals the importance of calibrating the 2010 imagery to the image conditions (i.e., film sensitivity, yellow filter, and difference in overall brightness) to the 1940 imagery (Figure 5). Replicating of the image conditions of the 1940 imagery to the 2010 imagery and calibrating the imagery to spectral reflectance, allowed for the comparison of image data sets for analysis. This step standardized the spectral reflectance range in intensity for both sets of imagery. Validation of these assumptions can be seen by observing the slope correction factors calculated for each image (Figure 5). The correction factors were within 3/1000 of one another showing that the image conditions for the 2010 imagery were almost identical to the 1940 imagery. The assumptions made in this study concerning the film sensitivity and yellow filter use for the 1940 imagery limited the spectral information available for analysis; however, they were necessary for comparison of habitat types both image data sets.

Classification Method

CV pixel values proved to be an effective reference for determining habitat types for Horn Island ca. 1940. Overall accuracies for the 2010 and 1940 imagery were 84.4% and 80.1%, successfully classifying six habitat types for a 21x21 window size. This suggests that the assumption that habitat structure has not changed over this 70 year

period is valid. If the overall accuracies had a greater difference it could be assumed that habitat structure has changed over a 70 year period. This would mean that the ranges of 2010 CV values used as reference for habitat types would have less of a chance of existing in 1940, making it apparent that certain habitat types do not exist anymore or have structural changed over time. The objective of creating a reliable, with at least an 80% accuracy, habitat map of Horn Island ca. 1940 is possible with only present day CV values and the spatial information.

ML Classification Overall Accuracies

The multi scale approach taken to analyze the 1940 imagery raises certain issues when considering accuracy at different window sizes. The data suggested multiple peaks in accuracies can occur with increasing window size. The peaks reveal the effects edge misclassification along transition areas between habitats. Research has shown that when using a multi scale texture approach issues arise with edges of textures transitioning into another texture; as the window crosses these boundaries, it analyzes the combination of the two different textures (Csillag & Kabos, 1996; Franklin, Wulder, & Gerylo, 2001; Coburn & Roberts, 2004; Kim, Warner, Madden, & Atkinson, 2011). Coburn and Roberts (2004) state that this edge effect is most apparent with increasing window size and can lead to the misclassification of the edges of texture features, particularly at the edges of spatially homogenous areas such as a body of water or bare sand. The peaks shown in the overall accuracy data show the effects of this phenomenon with decreasing accuracy as window size increases. This problem was addressed by looking at the commission and omission errors for each habitat at each different window size.

Analyzing the omission and commission errors within the confusion matrix was helpful in understanding why the 21x21 window size had the highest accuracies for both 2010 and 1940 (Table 3). Coburn and Roberts' (2004) research also observed local variance of an image at different window sizes and determined that smaller window sizes provided higher accuracies, to more homogenous areas, whereas larger window sizes provided higher accuracies for more heterogeneous areas. With this information it can be said that there is no optimal window size to classify habitat types for Horn Island.

Since smaller window sizes are better at representing more homogenous areas such as bare sand, water, and marsh habitats, lower commission and omission errors were expected for the smaller window sizes (i.e., 5x5, 11x11). This was particularly apparent in the bare sand habitat types for 1940 and 2010. However, the other habitat types (i.e., slash pine woodland, estuarine shrubland, dune herbland) are not homogenous and are better represented by the larger window sizes (i.e., 21x21, 31x31). The 31x31 window size was not used for classification due to the given lower accuracies (Table 3).

Percent Land Cover Change

Slash Pine Woodland, Estuarine Shrubland, and Dune Herbland Percent Land Cover Change. Slash pine woodland decreased in land cover by 16%. This would most likely be primarily due to Hurricane Katrina. A senior honors thesis at The University of Southern Mississippi concluded that there was an 80% slash pine mortality rate after Katrina (Hughes, 2008). Effects from the hurricane such as salt water intrusion and wind damage were the main causes of mortality. It is important to note that the 2010 imagery had large areas that were classified as estuarine shrubland that were formerly slash pine woodland. These areas had suffered severe wind damage evident in the cardinal

directional photos used for 2010 classification purposes. The land cover of the estuarine shrubland habitat type before Katrina is unknown; therefore, the 4% increase could be somewhat misleading since the amount of land cover for estuarine shrubland before Katina is not known. The dune herbland habitat has increased in land cover due to major storm events that cause the over wash of sand into the interior of the islands, covering habitats behind the primary dunes. These over washed areas eventually are populated by plant species that are in line with the successional patterns of barrier islands (Fahrig, Hayden, & Dolan, 1993; Stallins & Parker, 2003).

Bare Sand and Marsh. The reduction of the bare sand habitat type can be associated with land loss over the past century due to shipping channels being elongated, widened, and deepened, causing sediment to be trapped within the augmented channels. This sediment was then dredged and transported to offshore sights away from the barrier island chain, effectively starving the islands of sediment supply (Lucas & Carter, 2008; Morton, 2008; Otvos & Carter, 2008). The increase in marsh habitat can be attributed to the RSLR. The RSLR for Horn Island is around 7 mm yr^{-1} (Lucas & Carter, 2008). This means the sea-level has risen approximately 490 mm, just under half a meter. With this rise in sea-level the water table of the island has been pushed up making drier habitats wet and at a lower elevation with respect to the water table and the shore line (Brinson et al., 1995; Lucas & Carter, 2008).

RSLR and Hurricane effects on Horn Island's Ecosystem

The effects of RSLR and Hurricanes have caused major alterations to the ecosystem of Horn Island. Effects have led to changes in climax communities (i.e., slash pine woodland to estuarine shrubland) and changes in dominate habitat types (i.e., slash

pine woodland to marsh). Hurricane alterations are intermittent and have a direct effect on habitat types causing physical damage such as wind damage and over wash areas. Hurricane Katrina played a significant role in shifting climax communities based on the 80% slash pine mortality rate calculated (Hughes, 2008). A climax community species can be defined, for this study, as a habitat type that is the highest level of plant succession on Horn Island. This type of alteration is immediate and happens over a short time period unlike the effects of RSLR which are gradual and continuous. With the increase in land cover of marsh, it can be inferred that RSLR is changing the dynamics of Horn Island's fresh water lens, and the elevation of habitat types causing drier habitat types, which exist at higher in elevations, to transition in to habitat types found at lower elevations (Brinson et al., 1995).

Habitat Type Characteristics

In order to understand the meaning of these CV curves, it is necessary to realize what each habitat types' texture composition (i.e., texture properties). Texture properties are the elements that make up the spatial pattern presented by the pixels in the image i.e. (background, shadows, and, canopy). The background consists of mainly the soil type and any organic matter that may be on the ground at the time of the image being taken. The spatial variability between these texture properties can be seen by noting the CV histograms for a habitat type.

When analyzing the shape and peak of these histograms, it is important to understand that the variance and mean values at different window sizes is being used to represent a habitat type. The shape of the histogram is dependent on the size of the object or texture feature (Zucker et al., 1975). Zucker et al. (1975) give three examples of this

relationship: 1) When the window size is smaller than the object measured the larger consistent regions are detected resulting in a steep, narrow curve; 2) When the window size is comparable to the object or texture feature being measured the shape is more Gaussian like, and is centered on increasingly higher values; and 3) When the window size is much larger than the objects measured than the histogram decreases in size and becomes inconsistent (Zucker et al., 1975). The variance (sum of the squares) second order statistic calculated by the co-occurrence matrix show the local variation of occurrences within a given window size (Haralick & Shanmugam, 1973). So this texture measure determines the characteristic variation between texture properties. Regions with high CV values show areas of high variability between texture properties. These highly variable areas are characteristics that define the texture for a given habitat. When the differences in variation are considerably unalike, it means that texture properties are similar considering a brightness range of 0 to 242, meaning it takes more pixels (space) to reach the maximum mean CV. Therefore, a larger window size is needed to represent the texture of said habitat because areas of high variation are spatially spread out. When mean CV value differences are small, it means the texture properties are noticeably different, when considering a brightness range of 0 to 242 CV, and have higher variability between texture properties are spatially clustered, meaning less pixels (space) are needed to characterize the texture of said habitat type. Therefore, a smaller window is needed to denote the texture of said habitat type. When the texture is fully represented by the peak window size it can then be inferred that the peak window size is a distinct relative patch size of a habitat.

Slash Pine Woodland. When interpreting this type of habitat, shadows from tree canopies were a regular pattern, as well as the canopy itself with the dead pine needles and debris on the ground as a background were associated with the habitat. Causal observations show, when considering a brightness scale of 0 to 242, that these properties are considerably different. The shadows of the canopy are very dark, black. The tree canopies themselves are shades of grey layered with darker shades of grey with a somewhat rough texture that resembles clouds. The background of dead pine needles and debris are a very dark grey. A different scale is needed to determine the characteristic curve of the slash pine woodland due to the curve being so small. This habitat type, (Figure 10) shows a broad, more rounded, curve which peaks at the 45x45 window size. So texture properties for slash pine woodland are clustered. This texture composition causes a similar clumping of the slash pine woodland community on a habitat type scale.

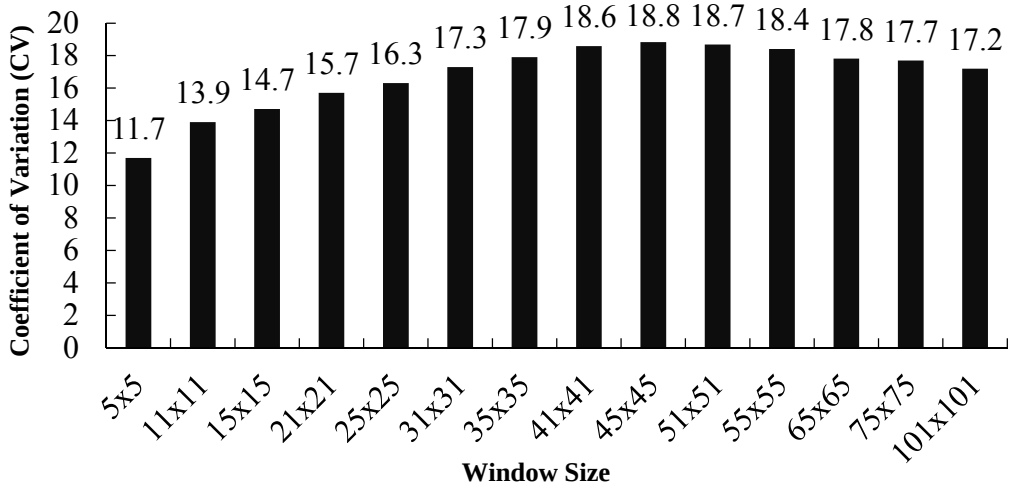

Figure 10. Slash pine woodland CV histogram. It can be seen that the 45x45 moving window is centered on the peak CV value.

Bare Sand. The bare sand habitat type showed little to know variation between window sizes. This was expected due to the composition of the sand on Horn Island. The sand is made of quartz, small amounts of black minerals. This is proof that using bare sand raw pixel values as a spectral reference to calibrate the image data sets works well for the standardization of BVs. The fact that there is little to no variation between windows sizes shows a regular, smooth, and evenly reflective surface allowing for well identified end members for the linear regression calibration.

Dune Herbland and Marsh. The CV curves for dune herbland and marsh are inconsistent with other habitat types (Figure 11 and 12). When calculating the larger window sizes, these habitat CV values were erratic and could not be calculated past the 101x101 window size. This is most likely due to window sizes analyzed being too large for texture properties such as habitat types to be characterized (Zucker et al., 1975). However, the CV values were not low and did not start to behave unpredictably until much larger window sizes. With this understanding it was realized that in order to characterize texture for marsh and dune herbland, imagery with a higher spatial resolution than one meter is needed.

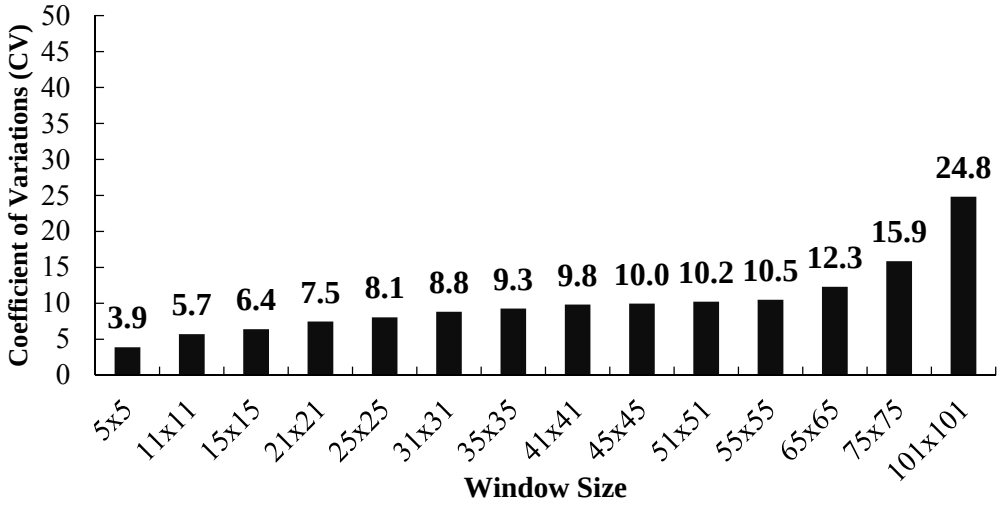

Figure 11. Dune herbland CV curve. Characterization was not possible due texture objects or highly variable area being smaller than one meter.

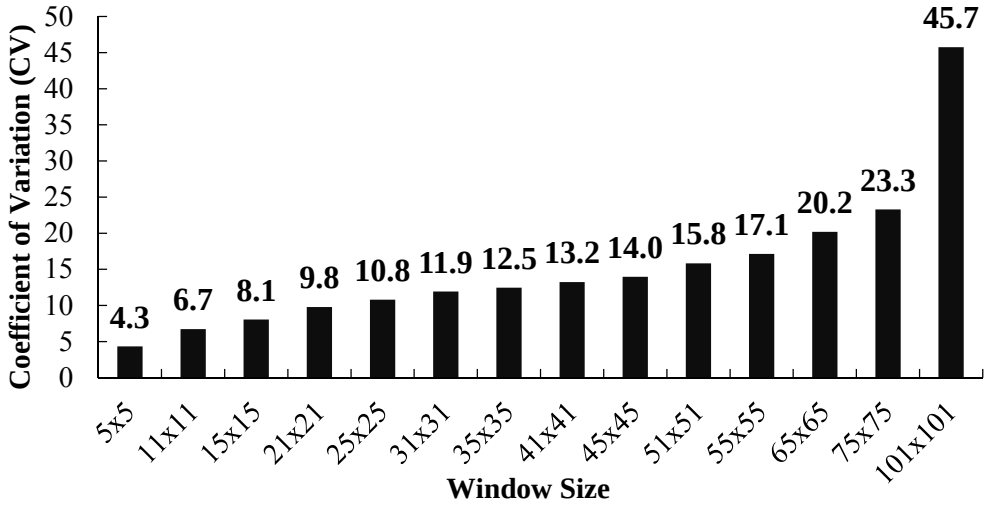

Figure 12. Marsh CV curve. The variations are too large to go any larger in window size and could not be calculated.

Estuarine shrubland. This habitat type was not able to be characterize most likely because the thresholds selected to represent the habitat were not precise and accurate enough to determine a characteristic texture. It is proposed that a tighter threshold be created to better represent this habitat type (Figure 13). Issues arise with estuarine

shrubland, because of the similarity in objects, or highly variable areas, to the marsh habitat types. The marsh habitat is actually two marsh habitat types low and high marsh. Low marsh is very homogenous with *Spartina alterniflora*, and high marsh is dominated by *Juncus roemerianus* which has a rougher more pronounced texture than low marsh resembling estuarine shrubland highly variable areas. These two habitat types were combined for classification purposes. If the range of CV values were smaller for this habitat type it could be suggested that the estuarine shrubland's curve would be a better representation of the characteristic dimension of relative patch size.

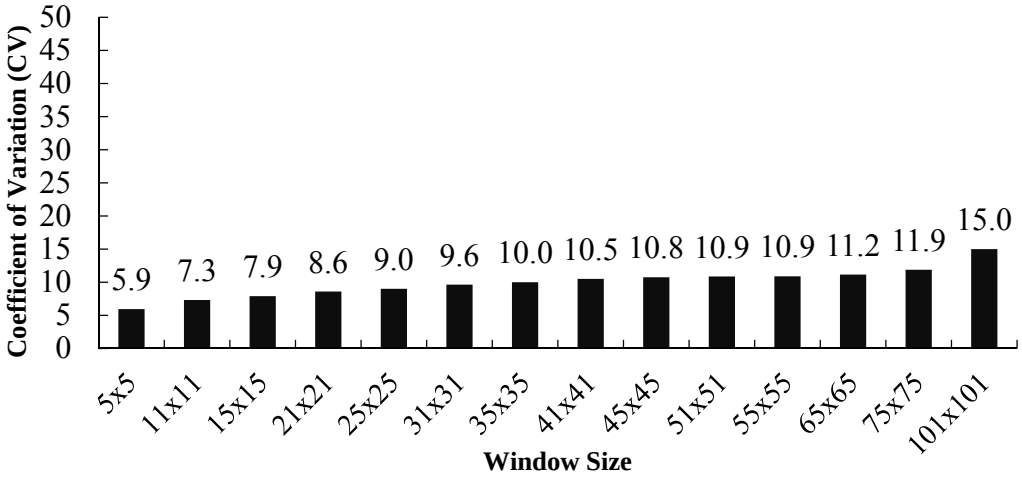

Figure 13. Estuarine shrubland CV curve. Variations were too large and could not be calculated. This is a function of the thresholds used not being precise enough for characterizing texture.

Summary

This study has proven the value of the spatial information available in historical black and white aerial photography. The characterization of past habitat types through image texture and geo-statistics (CV) were successful for Horn Island ca. 1940. A major factor in the success of this textural method was the calibration of the 2010 NAIP

imagery to the image conditions of the USGS 1940 image data set. By calibrating the 2010 imagery to the 1940 imagery comparisons could be made knowing that the image conditions of both image datasets were similar. By standardizing the brightness values of each image data set, the pixel values were normalized to spectral reflectance; therefore, statistics could be employed and an accurate texture analysis could be run. This research provided the earliest known habitat map of Horn Island ca. 1940. This habitat map gives insight to how vegetation has responded to rising sea-levels, as well as hurricanes over a seventy year period, revealing a small portion of Horn Island's life history.

REFERENCES

Adam, E.; Mutanga, O., & Rugege, D. (2010). Multispectral and hyperspectral remote sensing for identification and mapping of wetland vegetation: a review. *Wetlands Ecological Management, 18*, 281-296.

Arivazhagan, S., & Ganesan, L. (2003). Texture classification using wavelet transform. *Pattern Recognition Letters*, *24*(9-10), 1513-1521.

Baraldi, A., & Parmiggiani, F. (1995). An Investigation of the Textural Characteristics Associated with Gray Level Co-occurrence Matrix Statistical Parameters. *IEEE Transaction ON Geoscience and Remote Sensing*, *33*(2), 293-304.

Bharati, M.H., Liu, J.J., & MacGregor, J.F. (2004). Image texture analysis: methods and comparisons. *Chemometrics and Intelligent Laboratory Systems*, *72*(1), 57-71.

Brinson, M.M., Christioan, R.R., & Blum, L.K. (1995). Multiple States in the Sea-Level Induced Transition from Terrestrial Gorest to Estuary. *Estuaries*, *18*(4), 648-659.

Browning, D.M., Archer, S.R., Asner, G.P., McClaran, M.P., & Wessman, C.A., (2008). Woody Plants in Grasslands Post-Encroachment Stand Dynamics. *Ecological Applications*, *18*(4), 928-994.

Buddenbaum, H., Schlerf, M., & Hill, J. (2005). Classification of coniferous tree species and age classes using hyperspectral data and geo-statistical methods. *International Journal of Remote Sensing*, *26*(24), 5453-5465.

Cabanes, C., Cazenave, A., & Le Provost, C. (2001). Sea level rise during the last 40 years determined from satellite and in situ observations. *Science*, *26,* 840-842.

Cahoon, D.R., Hensel, P.F., Spencer, T., Reed, D.J., McKee, K.L., & Saintilan, N. (2006). Coastal Wetland Vulnerability to Relative Sea-Level Rise: Wetland

Elevation Trends and Process Controls. *Wetlands and Natural Resource Management Ecological Studies*, *190*, 271-292.

Caridade, C.M.R, Marcal, A.R.S., & Mendonc, T. (2008). The use of Texture for image classification of black and white air-photographs. *International Journal of Remote Sensing*, *29*(2), 593-607.

Carlson, T.N., & Arthur, S.T. (2000). The impact of land use- land cover changes due to urbanization on surface microclimate and hydrology: a satellite perspective. *Global and Planetary Change*, *25*, 49-65.

Carlucci, L. (1972). A formal system for texture languages. *Pattern Recognition*, *4*, 53-72.

Carter, G.A. (1993). Primary and Secondary Effects of the Water Content on the Spectral Reflectance of Leaves. *American Journal of Botany*, *80*(3), 231-243.

Carter, G.A., Cibula, W.G., & Miller, R.L. (1996). Narrow-band Reflectance Imagery Compared with Thermal Imagery for Early Detection of Plant Stress. *Journal of Plant Physiology*, *148*, 515-522.

Carter, G.A., Lucas, K.L., Biber, P.D., Criss, G.A., & Blossom, G.A. (2011). Historical changes in seagrass coverage on the Mississippi barrier islands, northern Gulf of Mexico, determined form vertical aerial imagery (1940-2007). *Geocarto International*, *SI 26* (8), 663-673.

Church, J.A., & White, N.J. (2006). A 20th century acceleration in global sea-level rise. *Geophysical Research Letters*, *33*, 1-4.

Coburn, C.A., & Roberts, A.C.B. (2004). A multiscale texture analysis procedure for improved forest stand classification. *International Journal of Remote Sensing*, *25*(20), 4287-4308.

Cox, C., & Munk, W. (1954). Measurement of the Roughness of the Sea Surface from Photographs of the Sun's Glitter. *Journal of the Optical Society of America*, *44*(11), 838-849.

Crompton, J.L, Lee, S., & Shuster, T.J. (2001). A guide for undertaking economic impact studies: The Springfest example. *Journal of Travel Research*, 79-87.

Csillag, F., & Kabos, S. (1996). Hierarchal decomposition of variance with applications environmental mapping based on satellite images. *Mathematical Geology*, *28*, 385-405.

Davis Jr., R.A., & Hayes, M.O. (1984). What is a wave-dominated coast? *Marine Geology*, *60*(1-4), 313-329.

Day, J.W. Jr., Barras, J., Clairain, E., Johnston, J., Justic, D., Kemp, G.P., Ko, J.Y, Lane, R., Mitsch, W.J., Steyer, G., Templet, P., & Yanez-Arancibia, A. (2005). Implications of global climatic change and energy cost and availability for the restoration of the Mississippi delta. *Ecological Engineering*, *24*, 253-265.

Douglas, B.C., & Peltier, W.R. (2002). The puzzle of global sea-level rise. *Physics Today*, 35-40.

Eleuterius, L.N. (1979). A phytosociological study of Horn and Petit Bois Islands, Mississippi. *Coastal Field Research Laboratory, Southeast Regional Office, National Park Service, Final Report.*

Fahrig, L., Hayden, B., & Dolan, R. (1993). Distribution of Barrier Island Plants in Relation to Overwash Disturbance: A test of Life History Theory. *Journal of Coastal Research*, *9*(2), 403-412.

Fitzgerald, D.M., Fenster, M.S., Argow, B.A., & Buynevich, I.V. (2008). Coastal Impacts Due to Sea-Level Rise. *Annual Review of Earth and Planetary Sciences*, *36*, 601-647.

FitzGerald, D.M., Penland, S., Numedal, & Nummedal, D. (1984). Control of barrier island shape by inlet sediment bypassing: East Frisian Islands, West Germany, *Developments in Sedimentology*, *39*, 355-376.

Fonseca, M., & Bell, S. (1998). Influence of physical setting on seagrass landscapes near Beaufort, North Carolina, USA. *Marine Biology and Ecology*, *340*, 227-246.

Fonseca, M. (1996). The role of seagrass in near-shore sedimentary process: a review. *In*: K.F. Nordstromand C.T. Roman, eds. *Estuarine Shores: Evolution, Environments and Human Alterations*. London: John Wiley and Sons, 486.

Franklin, S. E., Wulder, M.A., & Gerylo, G.R. (2001). Texture Analysis of IKONOS panchromatic data for Douglas-fir forest age class separability in British Columbia. *International Journal of Remote Sensing*, *11*, 2627-2632.

Ge, S., Carruthers, Gong P., & Herrera, A. (2006). Texture Analysis For Mapping *Tamarix Parviflora* Using Aerial Photographs Along The Cache Creek, California. *Environmental Monitoring and Assesment, 114*, 65-83.

Haralick, R.M., & Shanmugam, K. (1973). Textural features for image classification. *IEEE Transactions on Systems, Man, and Cybernetics*, SMC-*3*(6), 610-621.

Haralick, R.M. (1979). Statistical and Structural Approaches to Texture. *Proceedings of the IEEE*, *67*(5), 786-804.

Hauta-Kasari, M., Parkkinen, J., Jaaskelainen, T., & Lenz R. (1999). Multi-spectral Texture Segmentation Based on the Spectral Co-occurrence Matrix. *Patterns and Analysis, 2,* 275-284.

Hayes, M.O. (1994). The Georgia Bight Barrier Island System. *In*: Davis, R.A., *Geology of Holocene Barrier Island Systems*, (eds.). New York: Springer Verlag, 233-304

Holgate, S.J., & Woodworth, P.L. (2004). Evidence of enhanced coastal sea level rise during the 1990s. *Geophysical Research Letters*, *31*(7), 1-4.

Honeycutt, C.E., & Plotnick, R. (2008). Image analysis techniques and grey-level co-occurrence matrices (GLCM) for calculating bioturbation indices and characterizing biogenic sedimentary structures. *Computers & Geosciences*, *34*(11), 1461-1472.

Horler, D.N., Dockray, M., & Barber, J. (1983a). The red edge of plant leaf reflectance. *International Journal of Remote Sensing*, *4*, 273-288.

Horler, D.N., Dockray, M., Barber, J., & Barringer, A.R. (1983b). Red edge measurements for remotely sensing plant chlorophyll content. *Advances in Space Research*, *3*, 273-277.

Hoyt, J.H. (1967). Barrier Island Formation. *Geological Society of America Bulletin*, *78*, 1125-1136.

Hoyt, J.H. (1968). Barrier Island formation: reply. *Geological Society of America Bulletin*, *82*, 1427-1431.

Hudak, A.T., & Wessman, C.A. (1998). Textural Analysis of historical aerial photography to characterize woody plant encroachment in South African savanna. *Remote Sensing of Environment*, *66*, 317-330.

Hudak, A.T., & Wessman, C.A. (2001). Textural analysis of high resolution imagery to quantify bush encroachment in Madijwe Game reserve, South Africa, 1955-1996. *International Journal of Remote Sensing*, *22*(14), 2731-2740

Hughes, J. (2008). *Tree Mortality on Horn Island following Hurricane Katrina*. Honors Senior Thesis. The University of Southern Mississippi.

Jensen, J.R. (2007). *Remote Sensing of the Environment: an earth resource perspective* (2nd eds.). London: Pearson Education Ltd.

Katz, A.H. (1948). Aerial Photographic Equipment and Applications to Reconnaissance. *Journal of the Optical Society of America*, *38*(7), 604-610.

Kim, M., Warner, T.A., Madden, M., & Atkinson, D.S. (2011). Multi-scale GEOBIA with very high spatial resolution digital aerial imagery: scale, texture and image objects. *International Journal of Remote Sensing*, *32*(10), 2825-2850.

Koch, E.W. (2001). Beyond light: physical, geological, and geochemical parameters as possible submersed aquatic vegetation habitat requirements. *Estuaries*, *24*, 1-17.

Koch, E.W., Sanford, L.P., & Chen, S.N. (2006). Waves in Seagrass Systems: Review and Technical Recommendations. *U.S. Army Corps of Engineers*.

Lu, D. & Weng, Q. (2005). Urban Classification Using Full Spectral Information of Landsat ETM+ Imagery in Marion County, Indiana. *Photogrammetric Engineering & Remote Sensing, 71*(11), 1275-1284.

Lucas, K.L., & Carter, G.A. (2008). The use of hyperspectral remote sensing to assess vascular plant species richness on Horn Island, Mississippi. *Remote Sensing of Environment, 112*(10), 3908-3915.

Lucas, K.L., & Carter, G.A. (2010). Decadal Changes in Habitat-Type Coverage on Horn Island, Mississippi, U.S.A. *Journal of Coastal Research*, *26*(6), 1142-1148.

Lucas, K.L., & Carter, G.A., (2013). Change in distribution and composition of vegetated habitats on Horn Island, Mississippi, northern Gulf of Mexico, in the initial five years following Hurricane Katrina. *Geomorphology*, *199*, 129-137.

Maenpaa, T., & Pietkainen, M. (2003). Mutli-scale Binary Patterns for Texture Analysis. *Image Analysis Lecture Notes in Computer Science*, *2749*, 885-892.

Materka, A., & Strzelecki, M. (1998). Texture Analysis Methods- A Review. *Technical University of Lodz, Institute of Electronics*, COST B11 report.

Mississippi Natural Heritage Program (2006). *Ecological Communities of Mississippi*. Retrieved from http://www.mdwfp.com/media/128362/plantwatchinglist.pdf

Morris, J.T., Sundareshwar, C., Nietch, T., Kjerfve, B., & Cahoon, D.C., (2002). Responses to Coastal Wetlands to Rising Sea Level. *Ecology*, *83*(10), 2869-2877.

Morton, R.A., & Sallenger, H., Jr. (2003). Morphological Impacts of Extreme Storms on Sandy Beaches and Barriers. *Journal of Coastal Research*, *19*(3), 560-573.

Morton, R.A. (2008). Historical changes in the Mississippi-Alabama barrier-island chain and the roles of extreme storms, sea level, and human activities. *Journal of Coastal Research*, *24*(6), 1587-1600.

Mudd, S.M., Howell, S.M., & Morris, J.T. (2009). Impact of dynamic feedbacks between sedimentation, sea-level rise, and biomass production on near-surface

marsh stratigraphy and carbon accumulation. *Estuarine, Coastal and Shelf Science*, *82*(3), 1-13.

Narashima Rao, P.V., Sesha Sai, M.V.R., Sreenivas, K., Krishna Rao, M.V., Roa, B.R.M., Dwivedi, S., & Venkataratnam,L. (2002)., Textural analysis of IRS-ID panchromatic data for land cover classification. *International Journal of Remote Sensing*, *23*(17), 3327-3345.

Oosting, H.J. (1954). Tolerance to salt spray of plant of coastal dunes. *Ecology*, *26*, 85-89.

Oertel, G.F. (1985). The barrier island system. *Marine Geology*, *63*, 1-18.

Otvos, E.G. (1981). Barrier island formation through near-shore aggradation-stratigraphic and field evidence. *Marine Geology*, *43*(3-4), 195-243.

Otvos, E.G. (1985). Barrier platforms: northern Gulf of Mexico. *Marine Geology*, *63*(1-4), 285-305.

Otvos, E.G. (1990). Mississippi and Adjacent Coastal Sectors; Geological and Environmental Perspectives. *In*: Long Term Implications of Sea Level Change for the Mississippi and Alabama Coastlines. *Proceedings of a Conference Presented in Biloxi, Mississippi September 27-28*, 57-67.

Otvos, E.G., & Carter, G.A. (2008). Hurricane degradation-barrier development cycles, northeastern Gulf of Mexico: landform evolution and island chain history. *Journal of Coastal Research*, *24*(2), 463-478.

Pacifici, F.; Chini, M., & Emery, W.J. (2009). A neural network approach using multi-scale textural metrics from very high-resolution panchromatic imagery for urban land-use classification. *Remote Sensing of Environment*, *113*(6), 1276-1292.

Partio, M., Cramariuc, B., Gabbouj, M., & Visa, A. (2002). Rock texture retrieval using gray level co-occurrence matrix. *Proceedings of 5th Nordic Signal Processing Symposium*.

Peneva, E., Griffith, J.A., & Carter, G.A. (2008). Seagrass Mapping in the Northern Gulf of Mexico using Airborne Hyperspectral Imagery: A Comparison of Classification Methods. *Journal of Coastal Research*, *24*(4), 850-856.

Penland, S., & Ramsey, K.E. (1990). Relative sea-level rise in Louisiana and the Gulf of Mexico: 1908-1988. *Journal of Coastal Research*, *6*(2), 323-342.

Penland, S., McBride, R.A., Williams, S.J., Boyd, R., & Suter, J.R. (1991). Effects of Sea Level Rise on the Mississippi River Delta Plain. *Coastal Sediments*, In Kraus, N.C., Gingerich, K.J., & Kriebel D.L., eds., Coastal Sediments. New York: American Society of Civil Engineering, 1248-1264.

Pentland, A.P. (1984). Fractal-Based Description of Natural Scenes. *IEEE Transactions on Pattern Analysis and Machine Intelligence*, PAMI-*6*(6), 661-674.

Pessin, L.J., & Burleigh, T.D. (1941). Notes on the Forest Biology of Horn Island, Mississippi. *Ecology*, *22*(1), 70-78.

Pilkey, O.H. (2003). *A celebration of the world's barrier islands*. New York: Columbia University Press.

Pohl, C., & Van Genderen, J.L. (1998). Multisensor image fusion in remote sensing: concepts, \methods and applications. *International Journal of remote Sensing*, *19*(5), 823-854.

Schwartz, M.L. (1971). The Multiple Causality of Barrier Islands. *The Journal of Geology*, I(1), 91-94.

Shallaby, A., & Tateishi, R. (2007). Remote sensing and GIS for mapping and monitoring land cover and land-use changes in the Northwestern coastal zone of Egypt. *Applied Geography*, *27*(1), 28-41.

Stallins, J.A., & Parker, A.J. (2003). The Influence of Complex Systems Interactions on Barrier Island Dune Vegetation Pattern and Process. *Association of American Geographers*, *93*(1), 13-29.

Stanley, D.J., & Warne, A.G. (1994). Worldwide initiation of Holocene marine deltas be deceleration of sea-level rise. *Science*, *8*(265) 228-231.

Stauble, D.K. (1989). Barrier islands-dynamic coastal landforms requiring complex management decisions, a symposium introduction and overview. *In*: Stauble, D.K. and Magoon, O.T. (eds), *Barrier Islands: Process and management.* New York: American Society of Civil Engineers, 63-77.

Stone, G.W., Liu, B., Pepper, D.A., & Wang, P. (2004). The importance of extratropical and tropical cyclones on the short-term evolution of barrier islands along the northern Gulf of Mexico, USA. *Marine Geology*, *210*, 63-78.

Stutz, M.L., & Pilkey, O.H. (2001). A review of global barrier island distribution. *Journal of Coastal Research*, *SI*, 694-707.

Stutz, M.L., & Pilkey, O.H. (2002). Global distribution and morphology of deltaic barrier island systems. *Journal of Coastal Research*, *SI 36*, 694-707.

Stutz, M.L., & Pilkey, O.H. (2011). Open-Ocean Barrier Islands: Global Influence of Climatic, Oceanographic, and Depositional Settings. *Journal of Coastal Research*, *27*(2), 207-222.

Swift, D.J.P. (1975). Barrier-island genesis: evidence form the central Atlantic shelf, eastern U.S.A. *Sedimentary Geology*, *14*(1), 1-43.

Tornqvists, T.E., Gonzalez, J.L, Newsom, L.A., van der Borg, K., de Jong, A.F.M., & Kurnik, C.W. (2004). Deciphering Holocene sea-level history on the U.S., Gulf Coast: A high resolution record form the Mississippi Delta. *Geological Society of America*, *116*(7/8), 1026-1039.

Van Gool, L., Dewaele, P., & Oosterlinck, A. (1985). Texture Analysis Anno 1983. *Computer Vision,Graphics, and Image Processing*, *29*, 336-357.

Vogelmann, J.E, Sohl, T., & Howard, S.M. (1998). Regional characterization of land cover using multiple sources of data. *Photogrammetric Engineering & Remote Sensing*, *64*(1), 45-57.

Wang, P., Kirby. J.H., Horwitz, M.H., Knorr, P.O., & Krock, J.R. (2006). Morphological and Sedimentological Impacts of Hurricane Ivan and Immediate Post storm Beach Recovery along the Northwestern Florida Barrier-Island Coasts. *Journal of Coastal Research*, *22*(6), 1982-1402.

Willis, J.K., Chambers, Kuo, C.Y., & Chum, C.K. (2010). Global sea level rise. *Oceanography*, *23*(4), 26-35.

Zucker, S.W., Rosenfeld, A., & Davis, L. (1975). Picture segmentation by texture discrimination. *IEEE, Transactions on Computers*, 1228-1233.